Experimental and Molecular Pathology 93 (2012) 237–245

Contents lists available at SciVerse ScienceDirect

Experimental and Molecular Pathology

journal homepage: www.elsevier.com/locate/yexmp

Nuclear localization of heme oxygenase-1 is associated with tumor progression of head and neck squamous cell carcinomas

Norberto A. Gandini [a], María E. Fermento [a], Débora G. Salomón [a], Jorge Blasco [b], Vyomesh Patel [c], J. Silvio Gutkind [c], Alfredo A. Molinolo [c], María M. Facchinetti [a], Alejandro C. Curino [a,*]

[a] Laboratorio de Biología del Cáncer, Instituto de Investigaciones Bioquímicas Bahía Blanca (INIBIBB-CONICET), Camino La Carrindanga Km. 7, 8000, Bahía Blanca, Argentina
[b] Servicio de Patología del Hospital Interzonal de Agudos Dr. José Penna, Avda. Lainez 2401, 8000, Bahía Blanca, Argentina
[c] Oral and Pharyngeal Cancer Branch, National Institute of Dental and Craniofacial Research, National Institutes of Health, 30 Convent Dr., Bethesda, MD, USA

ARTICLE INFO

Article history:
Received 26 September 2011
and in revised form 30 April 2012
Available online 8 May 2012

Keywords:
Heme oxygenase-1
Head and neck cancer
Tissue microarray

ABSTRACT

The expression of heme oxygenase-1 (HO-1) was shown to be increased in multiple tumors compared with their surrounding healthy tissues and was also observed to be up-regulated in oral squamous cell carcinomas (OSCC). However, conflicting results were obtained and little information is available regarding HO-1 significance in head and neck squamous cell carcinoma (HNSCC). Therefore, the aim of the present study was to perform a wide screening of HO-1 expression in a large collection of human primary HNSCCs and to correlate the results with clinical and pathological parameters. For this purpose, we investigated the expression of this protein by immunohistochemistry (IHC) in tissue microarrays (TMAs) of HNSCC and in an independent cohort of paraffin-embedded tumor specimens. HO-1 expression was further validated by real-time qPCR performed on selected laser capture-microdissected (LCM) oral tissue samples. Both the number of HO-1-positive samples and HO-1 immunoreactivity in the cancerous tissues were significantly higher than those in the non-tumor tissues. These results were confirmed at the mRNA level. Interestingly, HO-1 localization was observed in the nucleus, and the rate of nuclear HO-1 in HNSCC was higher than that in non-malignant tissues. Nuclear HO-1 was observed in HNSCC cell lines and increased even further following hemin treatment. Analysis of HO-1 expression and sub-cellular localization in a mouse model of squamous cell carcinoma (SCC) and in human HNSCC revealed that nuclear HO-1 increases with tumor progression. Taken together, these results demonstrate that HO-1 is up-regulated in HNSCC and that nuclear localization of HO-1 is associated with malignant progression in this tumor type.

Introduction

Heme oxygenase (HO) is a microsomal enzyme catalyzing the first rate-limiting step in heme degradation, leading to the formation of equimolar quantities of carbon monoxide (CO), to biliverdin, which is converted to bilirubin by biliverdin reductase, and to free iron, and playing an important role in the recycling of the latter. (De Matteis et al., 2002; Jozkowicz et al., 2007; Tenhunen et al., 1968). Only recently has it been recognized that these three products have important physiological roles. (Jozkowicz et al., 2007; Otterbein et al., 2000; Snyder and Baranano, 2001). Two distinct mammalian HO isoforms (HO-1 and HO-2) have been identified. HO-1, the inducible 32-kDa isoform, is a ubiquitous heat shock protein (HSP32) (Maines and Gibbs, 2005). HO-1 can be induced in response to cellular stress, oxidative stimuli and hypoxia, an important process frequently occurring during tumor growth. In contrast, HO-2 is a constitutively expressed 36-kDa protein (Was et al., 2010).

An increasing body of evidence indicates that HO-1 may play an important role in cancer. It has been suggested that eight hallmark capabilities and two enabling characteristics are necessary for a complete tumor formation and progression. The first eight capabilities are: sustaining proliferative signaling, evading growth suppressors, resisting cell death, enabling replicative immortality, inducing angiogenesis, reprogramming of energy metabolism, evading immune destruction and activating invasion and metastasis. The enabling characteristics are: genome instability and inflammation (Hanahan and Weinberg, 2000, 2011). There is evidence of HO-1 being related to most of these capabilities and to the two enabling characteristics (Jozkowicz et al., 2007; Was et al., 2010). Furthermore, HO-1 was reported to be up-regulated in the majority of the rat, mouse and human tumors analyzed (Jozkowicz et al., 2007; Was et al., 2010).

Abbreviations: HO-1, heme oxygenase-1; HNSCC, head and neck squamous cell carcinoma; TMA, tissue microarray; SCC, squamous cell carcinoma; OSCC, oral squamous cell carcinoma; LCM, laser capture microdissection; IHC, immunohistochemistry; IRS, semi-quantitative immunoreactive score.

* Corresponding author at: Laboratorio de Biología del Cáncer, Instituto de Investigaciones Bioquímicas Bahía Blanca (INIBIBB-CONICET), Centro Científico Tecnológico Bahía Blanca, Camino La Carrindanga Km. 7, C.C. 857, 8000 Bahía Blanca, Argentina. Fax: +54 291 4861200.
E-mail address: acurino@criba.edu.ar (A.C. Curino).

0014-4800/$ – see front matter © 2012 Elsevier Inc. All rights reserved.
doi:10.1016/j.yexmp.2012.05.001

Human HNSCC is one of the six most common cancers in the world with approximately 500,000 new cases each year (Parkin et al., 2005) and, despite advances in the understanding of this disease and improvements in diagnosis and treatment options, the 5-year survival rate remains considerably lower than that for other cancers (Jemal et al., 2008). In this regard, studies aimed at elucidating how the dysregulation of molecules contributes to HNSCC progression may help to identify new prognostic markers for the early diagnosis or response to treatment and, for this purpose, the knowledge regarding protein expression in tumors and its correlation with the patients' clinical data is relevant. In this context, only few studies have examined the expression of HO-1 in OSCC and its correlation with clinical pathological features (Lee et al., 2008a,b; Tsuji et al., 1999; Yanagawa et al., 2004). Furthermore, a polymorphism identified in the promoter region of HO-1 has been related to a higher risk of developing this type of carcinoma (Chang et al., 2004). However most of these studies were performed on a small number of tumor samples and, using only one technique, IHC, to detect HO-1. Moreover, conflicting results were obtained related to the association of HO-1 with lymph node metastasis and with the grade of differentiation of these tumors (Lee et al., 2008b; Tsuji et al., 1999; Yanagawa et al., 2004). All these studies were performed on OSCC and there are no data concerning the HO-1 expression in other HNSCCs. For these reasons, one of the objectives of this study was to investigate the expression of HO-1 by IHC using TMAs containing a large collection of HNSCC samples obtained from various anatomical localizations, and corroborate the HO-1 expression by quantification of mRNA obtained from selected laser capture-microdissected OSCC samples. HO-1 nuclear expression has been observed, as was the fact that this expression increased with the progression from moderate to severe oral epithelial dysplasia (Lee et al., 2008a). Related to this, HO-1 has been detected in the nucleus of mouse cell lines after exposure to hemin and hypoxia, showing that this localization is linked to the up-regulation of genes which protect the cells against oxidative stress (Lin et al., 2007). Furthermore, a study reported that HO-1 nuclear localization is associated with human prostate cancer (Sacca et al., 2007). In light of these results another objective of this study was to investigate the incidence of nuclear localization of HO-1 in HNSCC.

Methods

Tissue specimens

TMAs were constructed by the Head and Neck Cancer Tissue Array Initiative, Oral and Pharyngeal Cancer Branch, National Institute of Dental and Craniofacial Research, NIH (Molinolo et al., 2007) with IRB approval. Two different array blocks were used; one included tissues obtained from North and South America and South Africa, and the other block included tissues from Southeast Asian countries. Both blocks included a total of 225 HNSCC cases and 12 non-malignant head and neck tissues. Eighty-four tumors correspond to OSCC and 141 to extraoral HNSCC (pharynx, larynx and other locations). Additionally, 32 cores of non-malignant tissues (breast, placenta, colon, salivary glands, liver, lymph node, lung and skin) were included as controls. Data on the initial diagnosis, site, tumor grade, age and sex were collected. Three TMA slides of each array block were used in the analysis.

Additionally, a cohort of 33 independent tissue samples of HNSCC used as a validation set was analyzed in this retrospective study. These samples were retrieved from the Pathology Service of the Bahía Blanca Regional Hospital with IRB approval and were staged according to the American Joint Committee on Cancer (AJCC) staging system (Greene et al., 2002). They were procured from patients who had undergone surgical treatment between April 1998 and May 2004. These samples were well differentiated (WD; n = 3), moderately differentiated (MD; n = 14), poorly differentiated (PD; n = 14) and not determined (ND; n = 2), and stages II and III oral squamous cell carcinomas. None of the patients had received chemo- or radio-therapy before surgery. There were 28 samples from males and 5 from females with a median age of 61 (range 27–81). H&E staining was performed from each sample and the slides further re-evaluated by a pathologist (JB). The quality of each section was assessed, and certain slides were selected for quantitative evaluation based on successful fixation, proper orientation, and the presence of representative lesions. A series of 5-μm sections were cut from each sample and transferred onto polarized histological glass slides for further analysis.

Immunohistochemistry

IHC staining was performed as previously described (Facchinetti et al., 2010). In brief, slides were deparaffinized in xylene and rehydrated in a series of ethanol dilutions and water. They were incubated in 3% hydrogen peroxide to quench endogenous peroxidase. After washing in PBS, sections were blocked in 2% BSA in PBS. Sections were then incubated overnight at 4 °C with either primary rabbit anti-HO-1 antibody (SPA-896, Stressgen Bioreagents, Canada; dilution: 1:200) and primary goat anti-HO-1 antibody (M19, Santa Cruz Biotechnology; dilution 1:100), followed by incubation with diluted biotinylated secondary antibody and then incubation with VECTASTAIN ABC Reagent (Vector Laboratories Inc.). For negative controls, the primary antibodies were replaced with isotype specific IgG. Diaminobenzidine/H_2O_2 was used as a substrate for the immunoperoxidase reaction. They were lightly counterstained with hematoxylin, dehydrated through graded ethanol and xylene, and mounted with Permount (Fisher Scientific).

Histopathological evaluation of staining intensities and statistical analysis.

Immunostained sections were scored semiquantitatively based upon the proportion of tumor cells stained and the staining intensity, as previously described (Facchinetti et al., 2010). In brief, the specimens were assessed using the semi-quantitative immunoreactive score (IRS). The IRS was calculated by multiplying the staining intensity (graded as: 0 = no, 1 = weak, 2 = moderate and 3 = strong staining) and the percentage of positively stained cells (0 = less than 10% of stained cells, 1 = 11–50% of stained cells, 2 = 51–80% of stained cells and 3 = more than 81% of stained cells). The mean IRS for HO-1 in 10 randomly chosen fields of the individual IHC (400× magnification) was determined. In the TMA, only representative tissue cores containing at least 200 tumor cells were scored. Sections with an IRS of >0 were considered positive. Nuclear HO-1 staining was considered positive when at least 10% of the cells showed nuclear expression. All scores were entered into a standardized electronic spreadsheet (Excel for Microsoft Windows). The statistical significance of HO-1 expression between groups was determined by the two-tailed χ^2 test. All analyses were performed using SPSS 14 (SPSS Inc., Chicago, Ill., USA). p values of less than 0.05 indicated a significant result.

Laser capture microdissection

Slides containing frozen tissue sections belonging to 4 OSCC patients were fixed in 70% ethanol (30 s); after washing in ddH_2O, these were stained very briefly in Mayer's hematoxylin (10–15 s), followed by dehydration through graded ethanol (70–100%) and Safeclear II (xylene substitute; Fisher Diagnostics, Middletown, Va., USA). For LCM, stained uncovered slides that were thoroughly air dried were used. After locating the cells of interest, a CapSure LCM Cap (Applied Biosystems, Austin, Tex., USA) was placed over the target area and pulsed with laser to adhere cells to the cap; after sufficient capture (500–1000 cells), the cap was transferred to a 0.5-ml sterile microfuge tube containing RNA extraction buffer (Agilent RNA Micro-Isolation Kit; Agilent) for immediate processing, following the protocol provided by the manufacturer.

RNA amplification

Total RNA extracted from 500–1000 cells (10–50 ng) underwent two rounds of amplification using the MessageAmp II aRNA Amplification Kit (Applied Biosystems) and following the protocol provided. Briefly, each sample was reverse-transcribed with T7-oligo(dT) as the anchoring primer, and after the synthesis of the second-strand, the resulting cDNA underwent purification, and this was subsequently used as template for in vitro transcription using T7 polymerase to produce the first round aRNA. After purification, the resulting aRNA (300–500 ng) underwent an additional round of amplification to modify and prepare the product for downstream gene expression analysis. Essentially this modification involved reverse transcribing with T3N9 (1 μg/μl) anchoring primers and the in vitro transcription reaction with T3 polymerase, and collectively this resulted in an approximate 10,000-fold increase in the aRNA for most samples.

Quantitative real-time PCR

The expression of HO-1 was confirmed by real-time PCR analysis in normal oral mucosa and OSCC. Briefly, 1 μg of aRNA, isolated and amplified as described above was used as starting material, to which 1 μl (3 μg/μl) of random primers was added, and DEPC-treated water to total volume of 25 μl. The RNA mix was heated at 65 °C for 5 min and then chilled on ice. The other components were added to each RNA mix as follows; 10 μl of 5× first strand buffer, 5 μl of 0.1 M DTT, 1 μl of 25 mM dNTPs, 1 μl of ribonuclease inhibitor and 6 μl of DEPC-treated water. The samples were incubated at 42 °C for 2 min, followed by the addition of 1 μl of Superscript II (40 U/μl, Invitrogen, Inc) and incubated at 42 °C for 50 min. The reaction was inactivated at 70 °C for 5 min, followed by the addition of 1 μl (2U/μl) of Rnase H and incubation at 37 °C for 20 min. The resulting cDNA was used as substrate for qPCR reactions which were performed in the Bio-Rad iCycler, using Gene Expression Analysis software, and IQ SYBR Green Supermix (Bio-Rad Laboratories) according to the manufacturer's instruction. To assess relative gene expression the $2^{-\Delta\Delta Ct}$ method of relative quantification (Livak and Schmittgen, 2001) was applied. The following primer set was used: forward 5′-GGAACTGAGGATGCTGAAGG-3′; reverse 5′-AAGGAGGAAGGAGCCTATGG-3′. HPRT was used to normalize the quantitative data using the following primer set: forward 5′-TGGACAGGACTGAACGTCTTG-3; reverse 5′-CAGCAGGTCAGCAAAGAATTTA-3′.

Mouse skin tumor generation

Tumors were induced in 7 to 8 week-old SENCAR mice using a one-time 7,12-dimethyl benz(*a*)-anthracene (DMBA) treatment (5 μg) and repeated 12-O-tetradecanoylphorbol-13-acetate (TPA) treatments (2 μg) for 14 to 15 weeks as previously described (Darwiche et al., 2007; Hennings et al., 1985). Papillomas were collected after 14 to 15 weeks of promotion whereas squamous cell carcinomas were harvested as they appeared.

Immunofluorescence

Immunofluorescence was performed as previously described (Fermento et al., 2010). In brief, HNSCC cell lines HN12 and HN13 were routinely maintained in Dulbecco's modified Eagle's medium (DMEM; Invitrogen) supplemented with 10% fetal bovine serum (Bioser, Argentina), 2 mM glutamine, 50 U/ml penicillin, and 0.05 mg/ml streptomycin. For the experiment they were plated on glass coverslips, treated for 20 h with 40 μM hemin or vehicle, then fixed with 4% paraformaldehyde in PBS and permeabilized with 0.1% Triton X-100 in PBS for 10 min, followed by incubation with blocking solution (1% BSA in PBS). The antibody employed was the primary rabbit anti-HO-1 antibody (SPA-896, Stressgen Bioreagents, Canada; dilution: 1:400). After incubation with primary antibody, cells were incubated with anti-rabbit Alexa566 fluoro-conjugated antibodies (Molecular Probes, Invitrogen). The coverslips were washed with PBS and nuclei were stained with DAPI and then mounted on slides with ProLong Gold anti-fade reagent (Invitrogen). Images were captured with an Axiovert 200 M fluorescence microscope (Zeiss), equipped with an AxioCam MRm camera. Counting of 200 cells in 40× random fields was performed in order to study the proportion of cells containing nuclear HO-1, and then the rate of nuclear HO-1 in controls was compared with hemin-treated cells.

Results

Screening of HO-1 expression in human HNSCC tissue microarray

To screen widely for HO-1 protein expression in human HNSCC samples, we performed HO-1 IHC on TMAs consisting of HNSCC samples from eight different countries. The antibody used for HO-1 was first tested in relevant samples of HNSCC to confirm its applicability to paraffin-embedded tissues and to set up optimal conditions as well. No staining was observed when substituting the HO-1 antibody with a non-immune, isotype-matched IgG. Subsequently, we performed IHC on the TMAs and evaluated the staining pattern as explained in Methods. The combined material analyzed included 225 squamous cell carcinomas derived from tongue (n = 38), gingiva (n = 14), oral floor (n = 13), buccal mucosa (n = 19), oropharynx (n = 12), or from other extraoral HNSCC (n = 129) (Table 1). The normal oral tissues analyzed included floor of mouth (n = 11) and tongue (n = 1). Also, 32 cores of non-malignant tissues from different organs were used as controls. HO-1 protein was expressed at various levels in the tumors examined (representative selected array cores are shown in Fig. 1). The immunodetection of HO-1 disclosed a strong classical cytoplasmic staining (Figs. 1A and B, black arrows) in most tumor cells, while only some stromal cells expressed weak HO-1 staining (arrowhead). Interestingly, nuclear staining was observed in many of the samples (Figs. 1C and D, red arrows). Non-malignant oral tissues presented either negative or very low cytoplasmic HO-1 staining (Fig. 1E). From a total of 225 cores evaluated, 201 (89.3%) showed positive staining. The HO-1 expression levels were significantly higher in HNSCCs compared with normal oral tissues (p = 0.003).

Table 1
Correlation of HO-1 expression with clinico-pathological features. HO-1 expression, as assessed by IHC performed in the HNSCC tissue microarrays, was correlated with a number of clinico-pathological features such as age, gender, histological grade and tumor location. Protein expression was evaluated as described in the Methods section.

Characteristic	Total cases	Positive HO-1 (%)	Negative HO-1 (%)	p value
Age				
<60	76	70 (92.1)	6 (7.9)	
60–70	75	63 (84.0)	12 (16.0)	**0.19**
>70	74	68 (86.4)	6 (13.6)	
Gender				
Male	127	113 (89.0)	14 (11.0)	**0.84**
Female	98	88 (89.7)	10 (10.3)	
Histological grade				
WD	81	73 (90.1)	8 (9.9)	
MD	93	87 (93.5)	6 (6.5)	**0.02**
PD	45	35 (77.8)	10 (22.2)	
Nd	6	6 (100.0)	0 (0.0)	
Tumor site				
Gingiva	14	13 (92.8)	1 (7.2)	
Tongue	38	34 (89.5)	4 (10.5)	
Buccal mucosa	19	17 (89.5)	2 (10.5)	**0.08**
Oral floor	13	10 (76.9)	3 (23.1)	
Oropharynx	12	12 (100.0)	0 (0.0)	
Other	129	115 (89.1)	14 (10.9)	

Nd: not determined.

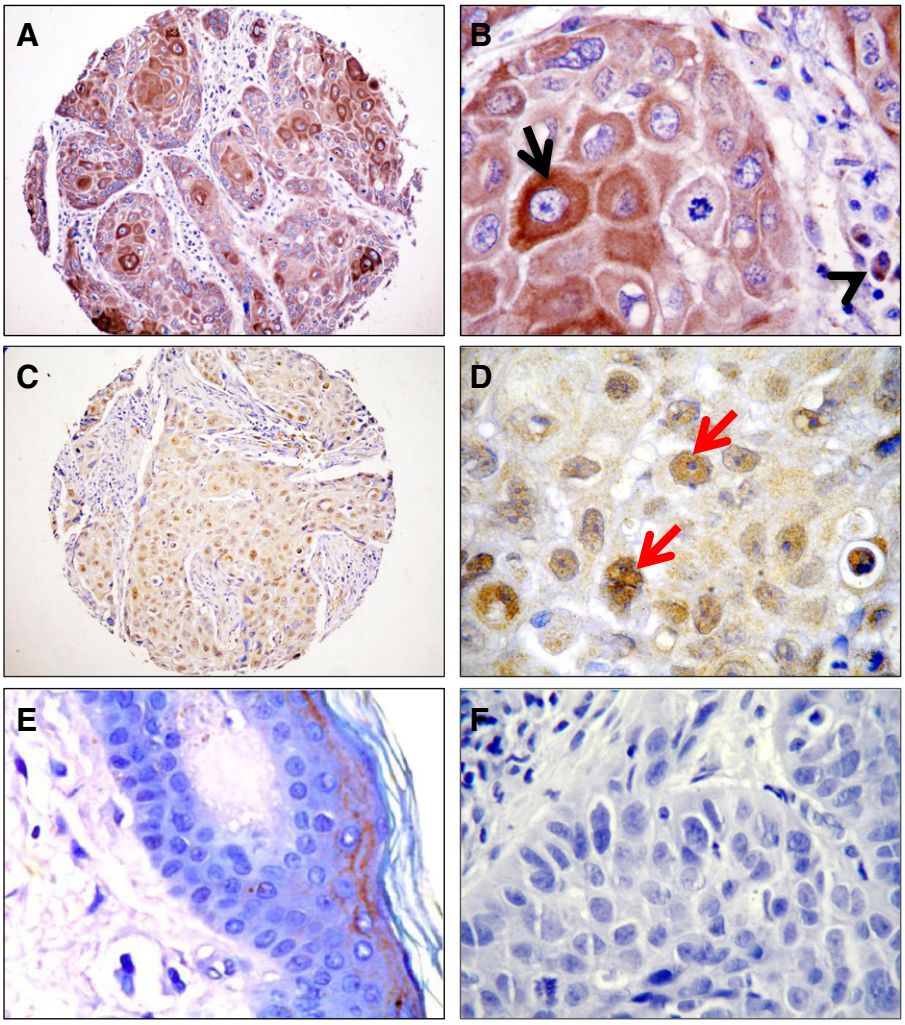

Fig. 1. Screening of HO-1 expression in HNSCC tissue microarrays (TMA). TMA slides were immunostained with HO-1 antibody, and evaluated semi-quantitatively as described in the Methods section. Representative TMA cores showing different levels of expression and the sub-cellular localization of the protein are included. A and B show cytoplasmic HO-1 and C and D show nuclear localization of the protein. E. A representative non-malignant tissue showing lack of HO-1 staining. F. A representative TMA core of a tumor section incubated with isotype-matched IgG, showing lack of staining. Original magnifications: 200× (A and C), 400× (E) and 1000× (B, D and F).

The immunohistochemical staining was also examined for correlation with a number of clinicopathological parameters (Table 1), namely, age, gender, histological grade, and tumor site. There were significant correlations between HO-1 expression and histological grade ($p = 0.02$), with well-differentiated and moderately-differentiated tumors displaying higher rates of HO-1 positivity. We found no significant association with age ($p = 0.19$), gender ($p = 0.84$), or tumor site ($p = 0.08$).

Analysis of HO-1 mRNA by RT-qPCR

In order to perform an independent comparison analysis of HO-1 expression between HNSCC and normal adjacent tissue using a different technique, selected samples belonging to four patients were micro-dissected by LCM. This allowed us to take pure samples of tumor and adjacent normal epithelium, and so prevent contamination with the other tissues. Tumor and adjacent oral tissue belonging to each patient were micro-dissected, RNA was extracted and HO-1 mRNA quantified by quantitative real-time PCR analysis. As shown in Fig. 2, increased expression of HO-1 mRNA was observed in tumor cells when compared with adjacent normal tissue ($p = 0.001$).

HO-1 is localized to nuclei in human HNSCC malignant tissues

Tissue microarrays allow the screening of molecules in a large collection of normal and tumor tissues simultaneously, a task which would be tedious with conventional molecular pathology technologies.

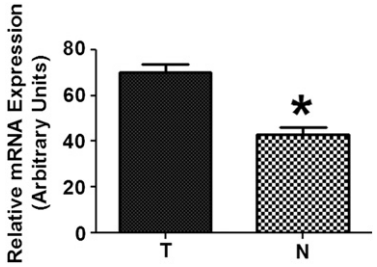

Fig. 2. HO-1 mRNA expression in OSCC is higher in malignant epithelia than in adjacent normal mucosa. Total RNA was prepared from cancerous or non-malignant epithelial tissues obtained by laser capture micro-dissection of samples belonging to four OSCC patients, reverse-transcribed, and subjected to qPCR using oligonucleotide primers specific for HO-1. The HO-1 expression was normalized using HPRT expression as an internal standard. Relative means ± SEM from HO-1 mRNA obtained from the patients' tumor tissues (T) and normal adjacent tissues (N) are shown ($p = 0.001$).

However the qualitative information concerning patterns of expression in tumor cells and normal tissue that can be obtained with TMAs is limited. We therefore examined the distribution of HO-1 in individual paraffin-embedded tissue sections obtained from surgically resected biopsies. Thirty three blocks were obtained from the pathology service of the Bahía Blanca Regional Hospital along with the patient's clinical data, and analyzed for HO-1 expression. The samples analyzed included pharynx (3), larynx (21), oral cavity (5), and other locations (4). Thirty tumor samples (91.0%) showed expression of HO-1 while no staining was observed in 3 samples (9.0%). In the non-malignant adjacent tissues lack of, or very low HO-1 cytoplasmic staining was observed. Comparison of tumor epithelial cells with non-malignant adjacent areas revealed significant differences in HO-1 staining intensity (Fig. 3A; $p = 0.002$). Fig. 3B shows an area of the malignant epithelia and Fig. 3C shows the adjacent area displaying low expression of HO-1. Only the cells of the basal layer showed positive expression of HO-1 in tumor adjacent areas and this expression was mainly cytoplasmic, with very few cells showing weak nuclear expression (black arrow, Fig. 3D). However, analysis of the sub-cellular localization of HO-1 showed that the nuclear localization was strongly increased in the malignant cells (Fig. 3B), as observed in the TMAs (Figs. 1C and D). Twenty-one out of 30 (70.0%) positive tumor specimens from HNSCC

Table 2
Correlation of HO-1 nuclear localization with histological grade in individual HNSCC samples. HO-1 sub-cellular localization, as assessed by IHC performed in the HNSCC individual samples was evaluated as described in the Methods section and correlated with the histological grade.

	Total positive cases	Nu/Cyt HO-1 (%)	Cyt HO-1 (%)
WD	3	1 (33.3)	2 (66.7)
MD	13	7 (53.8)	6 (46.2)
PD	14	13 (92.9)	1 (7.1)

Nu: nuclear; Cyt: cytoplasmic; χ^2: $p = 0.03$.

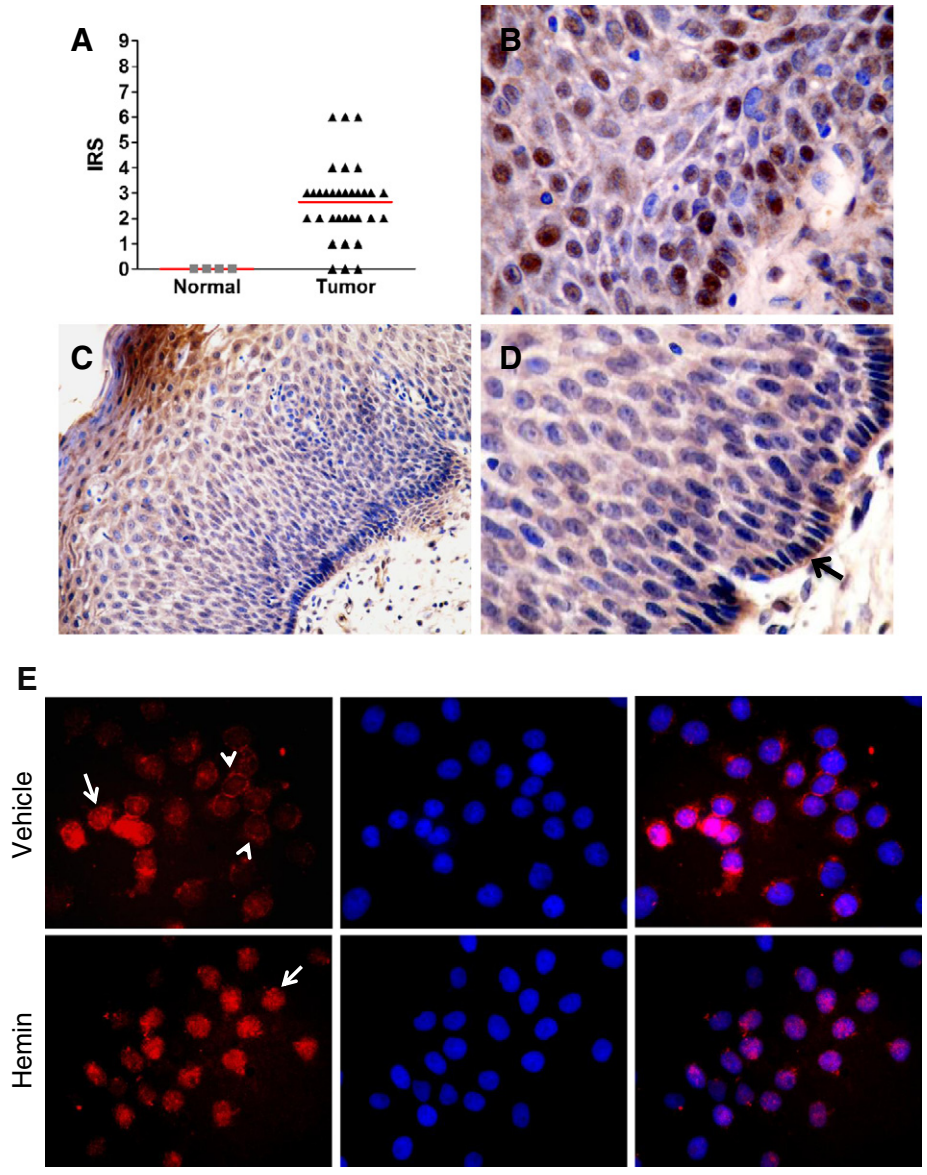

Fig. 3. Tumor epithelia show higher expression of nuclear HO-1 than non-malignant adjacent areas. Nuclear HO-1 is also observed in HN12 cell line. IHC for HO-1 was performed on the HNSCC individual samples and protein sub-cellular localization was evaluated as described in the Methods section. A. Dot plot showing differences in HO-1 expression between tumor and non-malignant oral tissue samples. B. Nuclear HO-1 staining is observed in malignant epithelia. C. Low HO-1 cytoplasmic staining in an adjacent area to the tumor specimen shown in B. D. Amplification of non-malignant tissue from C showing that cells of the basal layer are positive for HO-1 (black arrow). Original magnifications: 200× (C) and 1000× (B and D). E. IF for HO-1 in HN12 cell line showing both cytoplasmic (arrowhead) and nuclear (arrow) localization of HO-1. Nuclear localization increases following hemin treatment for 24 h. Original magnifications, 400×.

Table 3
Correlation of HO-1 nuclear localization with histological grade in TMAs. HO-1 subcellular localization, as assessed by IHC performed in HNSCC tissue microarrays was evaluated as described in the Methods section and correlated with the histological grade.

	Total positive cases	Nu/Cyt HO-1 (%)	Cyt HO-1(%)
WD	73	23 (31.5)	50 (68.5)
MD	87	22 (25.3)	65 (74.7)
PD	35	19 (54.3)	16 (45.7)
ND	6	1 (16.7)	5 (83.3)

Nu: nuclear; Cyt: cytoplasmic; χ^2: $p = 0.005$.

patients presented HO-1 nuclear localization. The rate of nuclear HO-1 expression was significantly higher in tumor epithelia than in epithelial cells of adjacent non-malignant tissues ($p = 0.03$). Furthermore, an association between HO-1 nuclear localization and histological grade was observed ($p = 0.03$; Table 2). Poorly differentiated tumors displayed higher percentages of nuclear HO-1. Analysis of the correlation of nuclear HO-1 with histological grade was also performed in TMAs and similar results were obtained ($p = 0.005$; Table 3).

In order to obtain more evidence of the nuclear expression of HO-1 in HNSCC and to investigate if this localization is increased by hemin activation as reported (Lin et al., 2007; Sacca et al., 2007), we further studied HO-1 sub-cellular localization in the HNSCC cell lines HN12 and HN13 by immunofluorescence. We observed nuclear localization of HO-1 in 30% (60 ± 12) of the cells whereas 70% (140 ± 20) of them presented perinuclear staining. Fig. 3E shows a representative picture showing nuclear (arrow) and perinuclear (arrowhead) HO-1 in HN12. Interestingly, upon hemin activation, 70% of the cells displayed nuclear HO-1 (Fig. 3E). Similar results were obtained for HN13 cell lines (data not shown).

Since it has been reported that HO-1 is proteolytically cleaved in its C terminus before translocating to the nucleus (Lin et al., 2007), we used the M19 antibody directed toward the C terminus of HO-1 in order to test if immunoreactivity was lost in the nuclei of the cells. As shown in Fig. 4, nuclear localization was clearly observed when using SPA-896 antibody, but was detected only in the cytoplasm of a consecutive section of the same tumor when M19 antibody was employed.

Nuclear HO-1 correlates with malignant progression in an animal model of SCC

The results obtained from human HNSCC suggest that HO-1 total expression augments in tumor tissues and HO-1 nuclear localization increases with tumor progression and aggressiveness. In order to further investigate this association between HO-1 and progression in SCC we analyzed its expression and sub-cellular localization in the classical mouse model of chemically induced skin carcinogenesis where the multiple stages of cancer development are readily accessible. For this purpose, we examined HO-1 expression by IHC in samples of normal skin, low risk papillomas, high risk papillomas, and squamous cell carcinomas generated by a DMBA-TPA chemical carcinogenesis protocol. All the tumors examined presented HO-1 expression. As expected, compared with normal skin where it was almost undetectable (Fig. 5A), HO-1 gradually increased in low risk papillomas (Fig. 5B), high risk papillomas (Fig. 5C) and SCC (Fig. 5D). Interestingly, HO-1 was localized to nuclei in malignant epithelial cells in the carcinoma (Fig. 5D) but was mainly cytoplasmic in normal skin and papillomas, further demonstrating that nuclear localization of HO-1 is associated with malignant progression.

Discussion

In this study we have shown that HO-1 is expressed in the majority of human HNSCCs, and this was demonstrated using both a TMA with hundreds of cancer tissue cores (89.3% of which were positive for HO-1) and an independent cohort of 33 tumor samples (91.0% positive samples). It was also observed that HO-1 expression is almost undetectable in normal tissue, increases slightly in non-malignant adjacent tissue and shows stronger expression in tumors. These results are in agreement with previous studies of the HO-1 expression in OSCC. In three of these studies HO-1 expression was observed in all the tumors examined (Lee et al., 2008b; Tsuji et al., 1999; Yanagawa et al., 2004), and in another report, 75% of the carcinomas showed immunoreactivity for HO-1 (Lee et al., 2008a). In the two studies where normal tissues were analyzed HO-1 expression was significantly higher in tumor samples compared with normal epithelial specimens (Lee et al., 2008a,b).

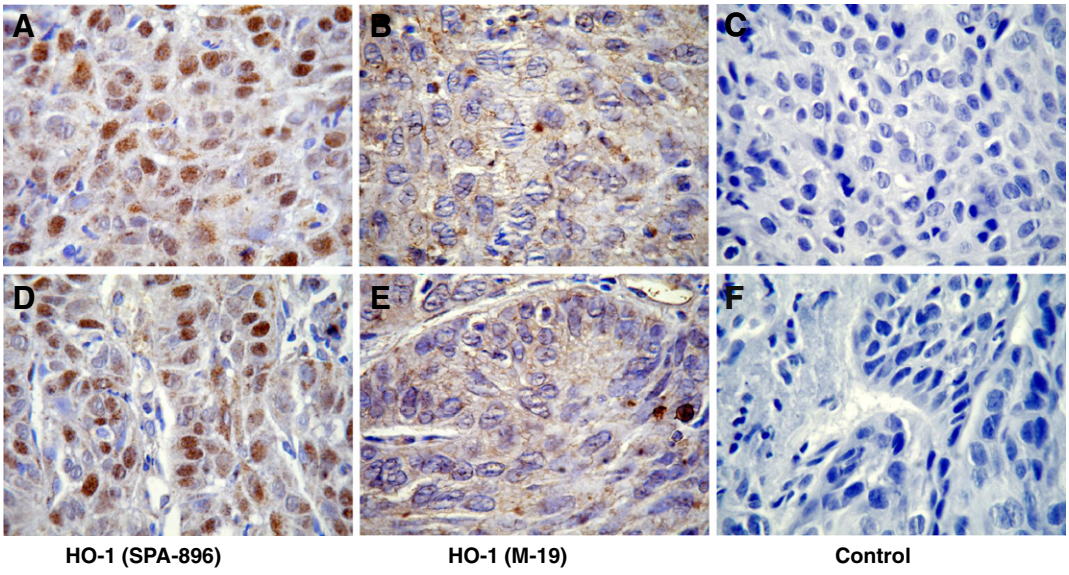

Fig. 4. Primary anti HO-1 antibody M19 raised against the C terminus of the protein does not stain nuclear HO-1. Two different tumors (A, B, C and D, E, F) were stained with SPA-896 antibody (A and D), with M19 antibody (B and E) and with no primary antibody as a control (C and F). Clear HO-1 nuclear localization can be observed in A and D whereas only cytoplasmic staining is observed in B and E. Original magnifications, 1000×.

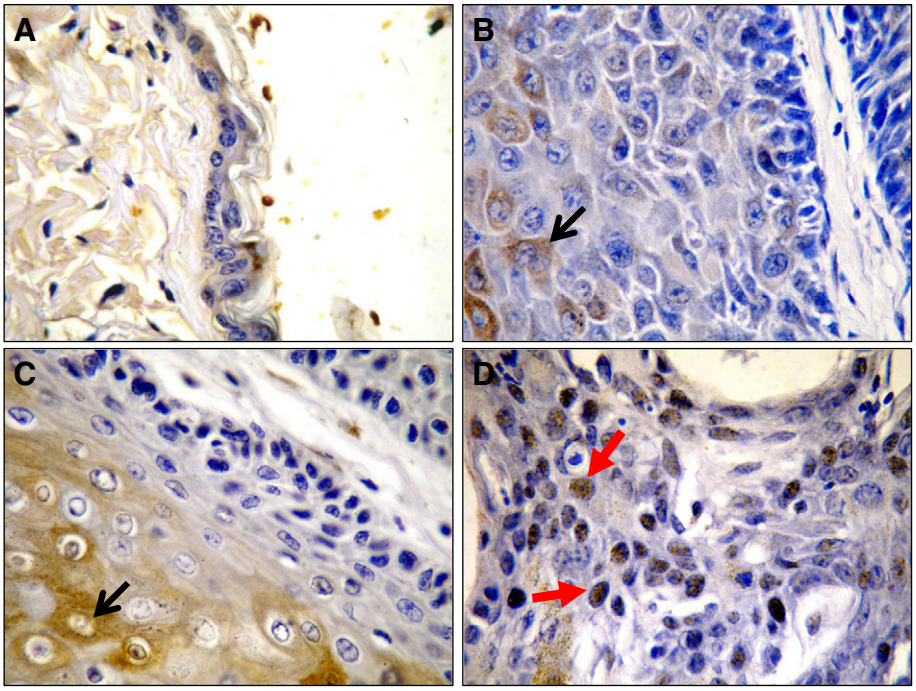

Fig. 5. Nuclear HO-1 correlates with malignant progression in a typical SCC murine model. Tissue sections from normal skin (A), papilloma low-risk (B), papilloma high-risk (C) and squamous cell carcinomas (D) were immunostained for HO-1 as described in the Methods section. Normal epithelial cells do not stain for HO-1 (A). Black arrows show HO-1 cytoplasmic localization in low-and high-risk tissues (B and C) and red arrows indicate nuclear localization for HO-1 in carcinomas (D). Original magnifications, 400×. (For interpretation of the references to color in this figure legend, the reader is referred to the web version of this article.)

Importantly, these results can now be generalized to all HNSCC whereas in previous studies only OSCC were analyzed. Also, in the previous studies HO-1 was detected only by IHC in tumor tissues. We were able to confirm this expression by using LCM combined with RT-qPCR. Indeed, our results are also coincident with previous studies of HO-1 expression in other types of cancers. Thus, HO-1 expression was reported to be strongly up-regulated in the majority of the rat, mouse and human tumors analyzed. This overexpression has been demonstrated in lymphosarcoma, (Schacter and Kurz, 1982), prostate carcinoma (Maines and Abrahamsson, 1996; Sacca et al., 2007), brain tumors, (Deininger et al., 2000; Hara et al., 1996), renal carcinoma (Goodman et al., 1997), hepatoma (Doi et al., 1999), melanoma (Torisu-Itakura et al., 2000), Kaposi sarcoma (McAllister et al., 2004), pancreatic cancer (Berberat et al., 2005) and in chronic myeloid leukemia (Mayerhofer et al., 2004). It has been reported that carriers of more active variants of the HO-1 promoter were more frequent among healthy subjects than among patients with OSCC in betel chewers (Chang et al., 2004). However, it has also been demonstrated in a mouse skin squamous cell carcinogenesis model that HO-1 protects healthy tissues against carcinogen-induced injury, but clearly induces malignant transformation in already growing tumors (Was et al., 2011). As already stated, other conflicting results were reported in previous studies of HO-1 expression in OSCC. In two of them low HO-1 expression was associated with lymph node metastasis and with low-to-moderately-differentiated tumors (Tsuji et al., 1999; Yanagawa et al., 2004). In another report, however, high HO-1 expression levels were associated with node metastasis and no significant differences were observed among the grade of differentiation in areca-quid-chewing-associated OSCC (Lee et al., 2008b). These contradictory results were ascribed to the different countries of origin of the specimens (Lee et al., 2008b). Contrary to these results we found higher HO-1 expression levels in more differentiated tumors. However, nuclear HO-1 localization showed a strong correlation with the grade of tumor differentiation. Importantly, the results we obtained in human HNSCC show that there is no expression of HO-1 in the nuclei of normal oral tissues, it is weakly expressed in the nuclei of epithelial cells of tumor adjacent areas and strongly expressed in the nuclei of the malignant cells of a subset of tumors. This nuclear expression was confirmed by immunofluorescence in two HNSCC cell lines and increased by hemin treatment. Furthermore, HO-1 nuclear expression was associated with less differentiated, more aggressive tumors. These results suggest that HO-1 nuclear localization is increased with tumor progression and is higher in more aggressive HNSCCs. This was confirmed in the typical mouse DMBA-TPA model of SCC. These results are coincident with a previous study showing that HO-1 nuclear staining increases in oral epithelial dysplasias when they progress from moderate to severe (Lee et al., 2008a). Similar results were also obtained in prostate cancer in which HO-1 nuclear expression was found to be lower in adjacent non-malignant tissues than in the prostate carcinoma ones where 65% of the samples showed nuclear localization of the enzyme (Sacca et al., 2007). Interestingly, HO-1 immunoreactive signal was also detected in the nucleus of cultured mouse cells after exposure to hypoxia and heme or heme/hemopexin (Lin et al., 2007). In the same report it was also shown that C-terminal cleavage was required for HO-1 nuclear transportation and that nuclear localization was associated with a reduction of the enzymatic activity. Accordingly, in human HNSCC we detected HO-1 nuclear and cytoplasmic expression using the SPA-896 anti-HO1 which is an N-terminal antibody, and only cytoplasmic HO-1 when we used an antibody specific for the C-terminal amino acids.

It has been suggested that nuclear HO-1 modulates key transcription factors involved in oxidative stress and cellular proliferation such as AP1 and NFκβ (Lin et al., 2007). There is evidence showing that HO-1 could have a physiological role independent of its enzymatic activity. For example, gene transfection of the activity-lacking mutant HO-1 protects cells against oxidative stress (Hori et al., 2002). Taken together, these results suggest that the HO-1 protein could have a role in the modulation of gene transcription. As the HO-1 structure does not show DNA-binding motifs it seems that this protein is not a typical transcription factor (Lin et

al., 2007). However, HO-1 may be able to modulate transcription factors, acting as a transcriptional co-regulator protein. It has been shown that HO-1 modulates most of the capabilities and enabling characteristics necessary for tumor initiation and progression. In this way, HO-1 has been related to modulation of cellular proliferation, apoptosis, angiogenesis, metastases, inflammation, immunosupression and oxidative injury, thus diminishing one of the endogenous causes of genetic instability (Jozkowicz et al., 2007; Was et al., 2010). It has been widely considered that either heme catabolites, such as biliverdin, bilirubin or carbon monoxide or the degradation of the pro-oxidant heme itself are responsible for the HO-1 physiological role. However, it is possible that HO-1 modulation of the cellular processes that are altered in cancer are, at least partially related to the HO-1 nuclear localization and its suggested role as a transcriptional co-regulator. Further research should be conducted to investigate if this nuclear localization of HO-1 has a cause–effect relationship in HNSCC. In conclusion we have shown that HO-1 mRNA and protein expression are strongly increased in human HNSCC tumors compared to adjacent non-malignant and normal tissues. Furthermore, we demonstrated an atypical nuclear localization of HO-1 in these tumors and in two human HNSCC cell lines. Importantly, this nuclear localization increases with tumor progression and correlates with less differentiated tumors.

Conflict of interest statement

The authors declare that there are no conflicts of interest.

Acknowledgments

This work was supported by the Agencia Nacional de Promocion Cientifica y Tecnológica (ANPCyT), the Comisión Nacional de Investigaciones Científicas y Técnicas (CONICET) and by the Universidad Nacional del Sur, Bahía Blanca, Buenos Aires, Argentina. Norberto A. Gandini is a recipient of a fellowship from CONICET and María E. Fermento is a recipient of a fellowship from Comisión de Investigaciones Científicas de la Provincia de Buenos Aires (CIC). We wish to acknowledge Dr Stuart Yuspa for providing the samples of the mouse model of SCC. Drs. Patel, Gutkind and Molinolo are supported by the Intramural Research Programme of the National Institute of Dental and Craniofacial Research, NIH.

References

Berberat, P.O., Dambrauskas, Z., Gulbinas, A., Giese, T., Giese, N., Künzli, B., Autschbach, F., Meuer, S., Büchler, M.W., Friess, H., 2005. Inhibition of heme oxygenase-1 increases responsiveness of pancreatic cancer cells to anticancer treatment. Clinical Cancer Research 11 (10), 3790–3798.

Chang, K.W., Lee, T.C., Yeh, W.I., Chung, M.Y., Liu, C.J., Chi, L.Y., Lin, S.C., 2004. Polymorphism in heme oxygenase-1 (HO-1) promoter is related to the risk of oral squamous cell carcinoma occurring on male areca chewers. British Journal of Cancer 91 (8), 1551–1555.

Darwiche, N., Ryscavage, A., Perez-Lorenzo, R., Wright, L., Bae, D.S., Hennings, H., Yuspa, S.H., Glick, A.B., 2007. Expression profile of skin papillomas with high cancer risk displays a unique genetic signature that clusters with squamous cell carcinomas and predicts risk for malignant conversion. Oncogene 26 (48), 6885–6895.

De Matteis, F., Dawson, S.J., Pons, N., Pipino, S., 2002. Bilirubin and uroporphyrinogen oxidation by induced cytochrome P4501A and cytochrome P4502B. Role of polyhalogenated biphenyls of different configuration. Biochemical Pharmacology 63 (4), 615–624.

Deininger, M.H., Meyermann, R., Trautmann, K., Duffner, F., Grote, E.H., Wickboldt, J., Schluesener, H.J., 2000. Heme oxygenase (HO)-1 expressing macrophages/microglial cells accumulate during oligodendroglioma progression. Brain Research 882 (1–2), 1–8.

Doi, K., Akaike, T., Fujii, S., Tanaka, S., Ikebe, N., Beppu, T., Shibahara, S., Ogawa, M., Maeda, H., 1999. Induction of haem oxygenase-1 nitric oxide and ischaemia in experimental solid tumours and implications for tumour growth. British Journal of Cancer 80 (12), 1945–1954.

Facchinetti, M.M., Gandini, N.A., Fermento, M.E., Sterin-Speziale, N.B., Ji, Y., Patel, V., Gutkind, S.J., Rivadulla, M.G., Curino, A.C., 2010. The expression of sphingosine kinase-1 in head and neck carcinoma. Cells, Tissues, Organs 192 (5), 314–324.

Fermento, M.E., Gandini, N.A., Lang, C.A., Perez, J.E., Maturi, H.V., Curino, A.C., Facchinetti, M.M., 2010. Intracellular distribution of p300 and its differential recruitment to aggresomes in breast cancer. Experimental and Molecular Pathology 88 (2), 256–264.

Goodman, A.I., Choudhury, M., daSilva, J.L., Schwartzman, M.L., Abraham, N.G., 1997. Overexpression of the heme oxygenase gene in renal cell carcinoma. Proceedings of the Society for Experimental Biology and Medicine 214, 54–61.

Greene, F.L., Page, D.L., Fleming, I.D., Fritz, A., Balch, C.M., 2002. AJCC Cancer Staging Manual, sixth ed. New York, Springer.

Hanahan, D., Weinberg, R.A., 2000. The hallmarks of cancer. Cell 100 (1), 57–70.

Hanahan, D., Weinberg, R.A., 2011. Hallmarks of cancer: the next generation. Cell 144 (5), 646–674.

Hara, E., Takahashi, K., Tominaga, T., Kumabe, T., Kayama, T., Suzuki, H., Fujita, H., Yoshimoto, T., Shirato, K., Shibahara, S., 1996. Expression of heme oxygenase and inducible nitric oxide synthase mRNA in human brain tumors. Biochemical and Biophysical Research Communications 224 (1), 153–158.

Hennings, H., Shores, R., Mitchell, P., Spangler, E.F., Yuspa, S.H., 1985. Induction of papillomas with a high probability of conversion to malignancy. Carcinogenesis 6 (11), 1607–1610.

Hori, R., Kashiba, M., Toma, T., Yachie, A., Goda, N., Makino, N., Soejima, A., Nagasawa, T., Nakabayashi, K., Suematsu, M., 2002. Gene transfection of H25A mutant heme oxygenase-1 protects cells against hydroperoxide-induced cytotoxicity. Journal of Biological Chemistry 277 (12), 10712–10718.

Jemal, A., Siegel, R., Ward, E., Hao, Y., Xu, J., Murray, T., Thun, M.J., 2008. Cancer statistics, 2008. CA: A Cancer Journal for Clinicians 58 (2), 71–96.

Jozkowicz, A., Was, H., Dulak, J., 2007. Heme oxygenase-1 in tumors: is it a false friend? Antioxidants & Redox Signaling 9 (12), 2099–2117.

Lee, J., Lee, S.K., Lee, B.U., Lee, H.J., Cho, N.P., Yoon, J.H., Choi, H.R., Lee, S.K., Kim, E.C., 2008a. Upregulation of heme oxygenase-1 in oral epithelial dysplasias. International Journal of Oral and Maxillofacial Surgery 37 (3), 287–292.

Lee, S.S., Yang, S.F., Tsai, C.H., Chou, M.C., Chou, M.Y., Chang, Y.C., 2008b. Upregulation of heme oxygenase-1 expression in areca-quid-chewing-associated oral squamous cell carcinoma. Journal of the Formosan Medical Association 107 (5), 355–363.

Lin, Q., Weis, S., Yang, G., Weng, Y.H., Helston, R., Rish, K., Smith, A., Bordner, J., Polte, T., Gaunitz, F., Dennery, P.A., 2007. Heme oxygenase-1 protein localizes to the nucleus and activates transcription factors important in oxidative stress. Journal of Biological Chemistry 282 (28), 20621–22033.

Livak, K.J., Schmittgen, T.D., 2001. Analysis of relative gene expression data using real-time quantitative PCR and the $^{2-\Delta\Delta CT}$ method. Methods 25 (4), 402–408.

Maines, M.D., Abrahamsson, P.A., 1996. Expression of heme oxygenase-1 (HSP32) in human prostate: normal, hyperplastic, and tumor tissue distribution. Urology 47 (5), 727–733.

Maines, M.D., Gibbs, P.E., 2005. 30 some years of heme oxygenase: from a "molecular wrecking ball" to a "mesmerizing" trigger of cellular events. Biochemical and Biophysical Research Communications 338 (1), 568–577.

Mayerhofer, M., Florian, S., Krauth, M.T., Aichberger, K.J., Bilban, M., Marculescu, R., Printz, D., Fritsch, G., Wagner, O., Selzer, E., Sperr, W.R., Valent, P., Sillaber, C., 2004. Identification of heme oxygenase-1 as a novel BCR/ABL-dependent survival factor in chronic myeloid leukemia. Cancer Research 64 (9), 3148–3154.

McAllister, S.C., Hansen, S.G., Ruhl, R.A., Raggo, C.M., DeFilippis, V.R., Greenspan, D., Früh, K., Moses, A.V., 2004. Kaposi sarcoma-associated herpesvirus (KSHV) induces heme oxygenase-1 expression and activity in KSHV-infected endothelial cells. Blood 103 (9), 3465–3473.

Molinolo, A.A., Hewitt, S.M., Amornphimoltham, P., Keelawat, S., Rangdaeng, S., Meneses García, A., Raimondi, A.R., Jufe, R., Itoiz, M., Gao, Y., Saranath, D., Kaleebi, G.S., Yoo, G.H., Leak, L., Myers, E.M., Shintani, S., Wong, D., Massey, H.D., Yeudall, W.A., Lonardo, F., Ensley, J., Gutkind, J.S., 2007. Dissecting the Akt/mammalian target of rapamycin signaling network: emerging results from the head and neck cancer tissue array initiative. Clinical Cancer Research 13 (17), 4964–4973.

Otterbein, L.E., Bach, F.H., Alam, J., Soares, M., Tao Lu, H., Wysk, M., Davis, R.J., Flavell, R.A., Choi, A.M., 2000. Carbon monoxide has anti-inflammatory effects involving the mitogen-activated protein kinase pathway. Nature Medicine 6 (4), 422–428.

Parkin, D.M., Bray, F., Ferlay, J., Pisani, P., 2005. Global cancer statistics, 2002. CA: A Cancer Journal for Clinicians 55 (2), 74–108.

Sacca, P., Meiss, R., Casas, G., Mazza, O., Calvo, J.C., Navone, N., Vazquez, E., 2007. Nuclear translocation of haeme oxygenase-1 is associated to prostate cancer. British Journal of Cancer 97 (12), 1683–1689.

Schacter, B.A., Kurz, P., 1982. Alterations in hepatic and splenic microsomal electron transport system components, drug metabolism, heme oxygenase activity, and cytochrome P-450 turnover in Murphy-Sturm lymphosarcoma-bearing rats. Cancer Research 42 (9), 3557–3564.

Snyder, S.H., Baranano, D.E., 2001. Heme oxygenase: a font with multiple messengers. Neuropsychopharmacology 25 (3), 294–298.

Tenhunen, R., Marver, H.S., Schmid, R., 1968. The enzymatic conversion of heme to bilirubin by microsomal heme oxygenase. Proceedings of the National Academy of Sciences of the United States of America 61 (2), 748–755.

Torisu-Itakura, H., Furue, M., Kuwano, M., Ono, M., 2000. Co-expression of thymidine phosphorylase and heme oxygenase-1 in macrophages in human malignant vertical growth melanomas. Japanese Journal of Cancer Research 91 (9), 906–910.

Tsuji, M.H., Yanagawa, T., Iwasa, S., Tabuchi, K., Onizawa, K., Bannai, S., Toyooka, H., Yoshida, H., 1999. Heme oxygenase-1 expression in oral squamous cell carcinoma as involved in lymph node metastasis. Cancer Letters 138 (1–2), 53–59.

Was, H., Dulak, J., Jozkowickz, A., 2010. Heme oxygenase-1 in tumor biology and therapy. Current Drug Targets 11 (12), 1551–15570.

Was, H., Sokolowska, M., Sierpniowska, A., Dominik, P., Skrzypek, K., Lackowska, B., Pratnicki, A., Grochot-Przeczek, A., Taha, H., Kotlinowski, J., Kozakowska, M., Mazan, A., Nowak, W., Muchova, L., Vitek, L., Ratajska, A., Dulak, J., Jozkowicz, A., 2011. Effects of heme oxygenase-1 on induction and development of chemically induced squamous cell carcinoma in mice. Free Radical Biology & Medicine 51 (9), 1717–1726, http://dx.doi.org/10.1016/j.freeradbiomed.2011.07.025.

Yanagawa, T., Omura, K., Harada, H., Nakaso, K., Iwasa, S., Koyama, Y., Onizawa, K., Yusa, H., Yoshida, H., 2004. Heme oxygenase-1 expression predicts cervical lymph node metastasis of tongue squamous cell carcinomas. Oral Oncology 40 (1), 21–27.